

Path Loss in Directional Antennas for 5G Millimeter-Wave Communications

Jyoti Dange · DR. R.P.Singh

Abstract: High data rate and huge bandwidth Millimeter wave systems suffer from poor link budget due to the blockage of the millimeter wave signal by the obstacles. Directional antenna which guarantees signal delivery if line of sight communication between the transmitter and receiver exists with the improvement in a signal strength. Multi Input Multi Output (MIMO) beamforming uses channel statistics to guide the beam improving the multiplexing gain and beamforming gain.

In this paper, Evaluation of the equivalent omnidirectional antenna pattern and omnidirectional received power are calculated by summing the received powers from all measured unique pointing angles received at antenna halfpower beamwidth step increments in the azimuth and elevation planes, By demonstrating that the synthesized omnidirectional received power and path loss this method is validated and are independent of antenna beamwidth, through theoretical analyses and millimeter-wave propagation measurements using antennas with different beamwidths. The method provide accurate results while increasing the measurement range substantially through the use of directional antennas.

Keywords: narrowbeam · path loss

I. INTRODUCTION

Millimeter-wave (mmWave) is considered as a promising technology for fifth generation (5G) mobile. High-gain directional antennas is use to overcome significant increase in free space path loss in mmWave frequencies at the base station and/or mobile handset sufficient gain to complete mmWave links over 500 m or so, For proper design of wireless systems and protocols MmWave propagation measurements are needed to accurately characterize channels and create statistical channel models.

Electrically-steerable adaptive antennas is used in 5G mmWave systems,

, many researchers are using mechanically rotatable horn antennas to measure the channel at a wide range of mmWave frequencies. Practical antennas like omnidirectional antennas in 5G mmWave systems is an alternative to electrically-steerable adaptive antennas [1], [7]–[9], as such antennas are not yet conveniently available for researchers at most mmWave frequencies, therefore many researchers are using mechanically rotatable horn antennas to measure the channel at a wide range of mmWave frequencies [1], [6], [10], [11].

II. RESULTS

To a measured set of data. it is a slope of the best fit line the slope is not the same as a PLE. The intercept α may be much higher than theoretical free space path loss at short distances and the slope β can be very close to zero or even negative, the measured data are so sparse or clustered in distance.

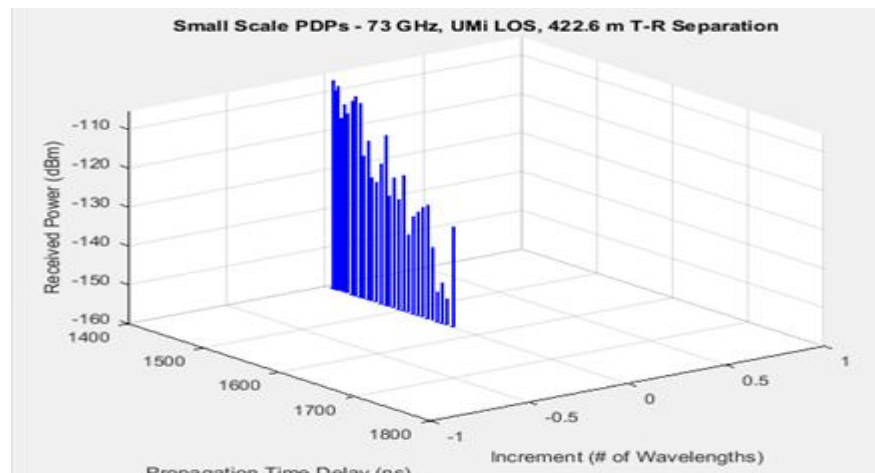


[Fig. 1 about here.]

Two parameters (α, β) in the FI model is opposed, by CI model which is more in a global manner robust for data sets as it considers only one path loss parameter n allows comparisons of results across different distances, environments, and research groups in a global manner. even in NLOS environments,

CI model makes physical sense because the first few meters from the transmitter will still be line-of-sight (LOS)(considering typical environments where the radio waves will propagate a number of meters before encountering the first obstacle) [4]. taking into account the LOS and NLOS probabilities, there is no difference between using the FI model and the 1 m CI model in NLOS environments when considering a probabilistic-type path loss model .taking into account the LOS and NLOS probabilities.

III. DISCUSSION

To study characteristics mmWave channel at 23 GHz using directional horn antennas at both the TX and RX at RF nullto-null bandwidth of 800 MHz multipath time resolution of 2.5 ns, which guarantees that a majority of multi- path components (MPCs) can be notable. In the 23 GHz measurements, three TX locations (heights of 7 m and 17 m) and 27 RX locations (heights of 1.5 m) were selected to conduct the measurements [4]. Two types of horn antennas were employed: a 24.5 dBi-gain narrowbeam horn antenna with 10.9° and 8.6 half-power beamwidths (HPBWs) in the azimuth and elevation planes, respectively, and a 15 dBi-gain wide beam horn antenna with 28.8 and 30 are selected are selected with HPBWs in the azimuth and elevation planes, respectively. At the TX locations The narrowbeam antenna was always utilized The narrowbeam antenna was always utilized at the TX locations, and five of the RX locations used both the narrowbeam and wide beam antennas, including two LOS and three NLOS locations At the TX locations The narrowbeam antenna was always utilized at the TX locations, and five of the RX locations used both the narrowbeam and widebeam antennas, including two LOS and three NLOS locations.

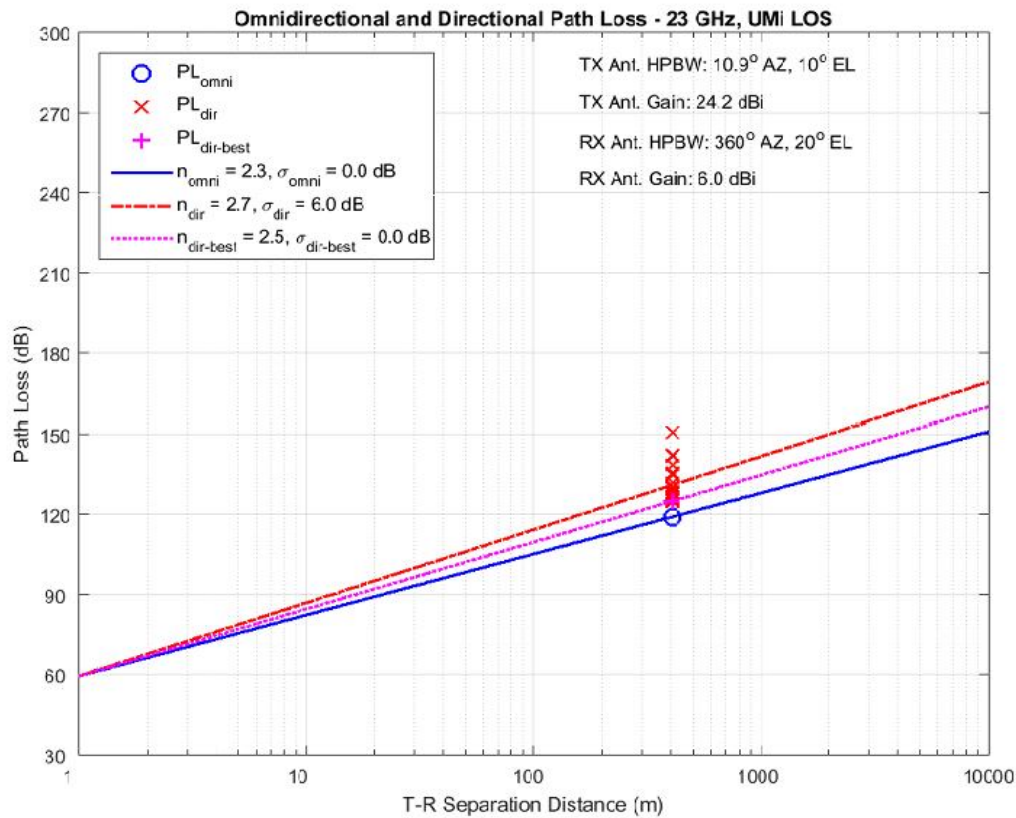


[Fig. 2 Omabouth here.]

For every TX-RX location combination (except the 2 LOS RX locations), the RX antenna was consecutive swept over the complete angle plane in increments of 1 HPBW at elevation angles of 0 and 20 concerning the horizon, so as to measure contiguous angular snapshots of the channel impulse response over the nine out of the ten measurement sweeps for each TX-RX location combination (except the two LOS RX locations),

The RX antenna was consecutive swept over the complete angle plane in increments of 1 HPBW at elevation angles of 0 and 20

concerning the horizon, so as to measure contiguous angular snapshots of the channel impulse response over the entire 360 azimuth plane, while the TX antenna remained at a fixed azimuth and elevation angle.

In the 73 GHz measurements, five TX locations (heights of 7 m and 17

m) and 27 RX locations were used, with RX antenna heights of 2 m (mobile scenario) and 4.06 m (backhaul scenario), yielding a total of 36 TX-RX location combinations for the mobile (access) scenario and 38 combinations for the backhaul scenario. A pair of 27 dBi-gain rotatable directional horn antennas with a HPBW of 7 in both azimuth and elevation planes was employed at the TX and RX. For each TX-RX location combination, TX and RX antenna azimuth sweeps were performed in steps of 8 or 10 at various elevation angles. In the measurement system, the total time of acquiring a power delay profile (PDP) (including recording and averaging 20 instantaneous PDPs) was $40.94 \text{ ms} \times 20 = 818.8 \text{ ms}$, where 40.94 ms was the time it took to record a single instantaneous PDP (The times were dilated based on the sliding correlation method) [4]. Additional measurement procedures, channel modeling results, and hardware specifications can be found in [1], [3], [4], [6].

IV. CONCLUSIONS

This paper presented and validated a method for synthesizing the omnidirectional antenna pattern and resulting omnidirectional received power and path loss from measured data using directional horn antennas, by summing the received powers from each and every measured non-overlapping directional

HPBW antenna pointing angle combination. Both theoretical analyses and measured results were provided to validate this method. It was shown that the received power using 3 narrowbeam antennas agreed relatively well with that received from a single widebeam antenna (where the

azimuth and elevation HPBWs of the widebeam antenna were about three times that of the narrowbeam antenna). Using directional antennas with different beamwidths yielded almost identical received power and path loss synthesized over a systematic incremental scan of the entire azimuth plane(s). By extrapolating these results between narrowbeam and widebeam antennas for the case of a complete azimuthal scan, it is shown that the omnidirectional antenna pattern may be synthesized through azimuthal and elevation scans over the entire 4 steradian sphere. In addition, the 73 GHz measurement data

Fig. 3. Comparison of 28 GHz NLOS effective directional path loss

using the widebeam (28.8 / 30 azimuth/elevation HPBW) and narrowbeam (10.9 / 8.6 azimuth/elevation HPBW) antennas at three RX locations. The “discrete” widebeam path loss is obtained using a single widebeam antenna, and the “discrete” narrowbeam path loss is synthesized from nine narrowbeam antennas with adjacent antennas separated by 10 and 20 in the azimuth and elevation planes, respectively. The “all” path loss corresponds to the effective path loss over the entire azimuth plane(s). showed that when considering the total

REFERENCES

- [1] T. S. Rappaport, S. Sun, R. Mayzus, H. Zhao, Y. Azar, K. Wang, G. N. Wong, J. K. Schulz, M. K. Samimi, and F. Gutierrez, Jr., “Millimeter Wave Mobile Communications for 5G Cellular: It Will Work!” *IEEE Access*, vol. 1, pp. 335–349, May 2013.
- [2] Z. Pi and F. Khan, “An introduction to millimeter-wave mobile broadband systems,” *IEEE Communications Magazine*, vol. 49, no. 6, pp.101–107, June 2011.
- [3] T. S. Rappaport, R. W. Heath, Jr., R. C. Daniels, and J. N. Murdock, *Millimeter Wave Wireless Communications*. Engwood Cliffs, NJ, USA: Pearson/Prentice Hall, 2015.
- [4] T. S. Rappaport, G. R. MacCartney, Jr., M. K. Samimi, and S. Sun, “Wideband millimeter-wave propagation measurements and channel models for future wireless communication system design (Invited Paper),” *IEEE Transactions on Communications*, vol. 63, no. 9, pp. 3029–3056, Sep. 2015.
- [5] T. S. Rappaport, W. Roh, and K. Cheun, “Mobile’s millimeter-wave makeover,” *IEEE Spectrum*, vol. 51, no. 9, pp. 34–58, Sep. 2014.
- [6] G. R. MacCartney, Jr. and T. S. Rappaport, “73 GHz millimeter wave propagation measurements for outdoor urban mobile and backhaul communications in New York City,” in 2014 IEEE International Conference on Communications (ICC), June 2014, pp. 4862–4867.
- [7] F. Gutierrez, S. Agarwal, K. Parrish, and T. S. Rappaport, “On-chip integrated antenna structures in CMOS for 60 GHz WPAN systems,” *IEEE Journal on Selected Areas in Communications*, vol. 27, no. 8, pp. 1367–1378, Oct. 2009.
- [8] H. Zhou, “Phased array for millimeter-wave mobile handset,” in 2014 IEEE Antennas and Propagation Society International Symposium (APSURSI), Jul. 2014, pp. 933–934.
- [9] W. Roh et al., “Millimeter-wave beamforming as an enabling technology for 5G cellular communications: theoretical feasibility and prototype results,” *IEEE Communications Magazine*, vol. 52, no. 2, pp. 106–113, Feb. 2014.
- [10] S. Hur et al., “Synchronous channel sounder using horn antenna and indoor measurements on 28 GHz,” in 2014 IEEE International Black Sea Conference on Communications and Networking (BlackSeaCom), May 2014, pp. 83–87.
- [11] S. Rajagopal et al., “Channel feasibility for outdoor non-line-of-sight mmwave mobile communication,” in *IEEE Vehicular Technology Conference (VTC Fall)*, Sep. 2012, pp. 1–6.
- [12] G. R. MacCartney, Jr., M. K. Samimi, and T. S. Rappaport, “Omnidirectional path loss models at 28 GHz and 73 GHz in New York City,” in 2014 IEEE International Symposium on Personal, Indoor and Mobile Radio Communications (PIMRC), Sep. 2014, pp. 227–231.
- [13] T. S. Rappaport, *Wireless Communications: Principles and Practice*, 2nd ed. Upper Saddle River, NJ: Prentice Hall, 2002.

[14] M. Hata, "Empirical formula for propagation loss in land mobile radio services," IEEE Transactions on Vehicular Technology, vol. 29, no. 3, pp. 317–325, Aug. 1980.

[15] J. B. Andersen, T. S. Rappaport, and S. Yoshida, "Propagation measurements and models for wireless communications channels," IEEE Communications Magazine, vol. 33, no. 1, pp. 42–49, Jan. 1995.

[16] P. Kyosti et al., "WINNER II channel models," European Commission, IST-WINNER, Tech. Rep. D1.1.2, Sept. 2007.

[17] 3GPP TR 25.996 V11.0.0, "Spatial channel model for multiple input multiple output (MIMO) simulations," Sep. 2012.

[18] G. R. MacCartney, Jr., J. Zhang, S. Nie, and T. S. Rappaport, "Path loss models for 5G millimeter wave propagation channels in urban microcells," in 2013 IEEE Global Communications Conference (GLOBECOM), Dec. 2013, pp. 3948–3953.

[19] A. I. Sulyman et al., "Radio propagation path loss models for 5G cellular networks in the 28 GHz and 38 GHz millimeter-wave bands," IEEE Communications Magazine, vol. 52, no. 9, pp. 78–86, Sep. 2014.

[20] M. K. Samimi, T. S. Rappaport, and G. R. MacCartney, Jr., "Probabilistic omnidirectional path loss models for millimeter-wave outdoor communications," IEEE Wireless Communications Letters, vol. 4, no. 4, pp. 357–360, Aug. 2015.

[21] Far field radiation from electric current. [Online]. Available: <http://www.thefouriertransform.com/applications/radiation.php>

LIST OF FIGURES

1 Small scale PDP-73GHZ 422.6m TR Separation..... 8

2 9

FIGURES

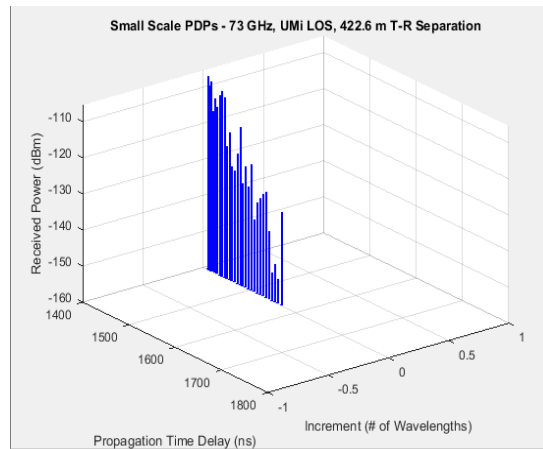


Fig. 1 Small scale PDP-73GHZ 422.6m TR Separation.

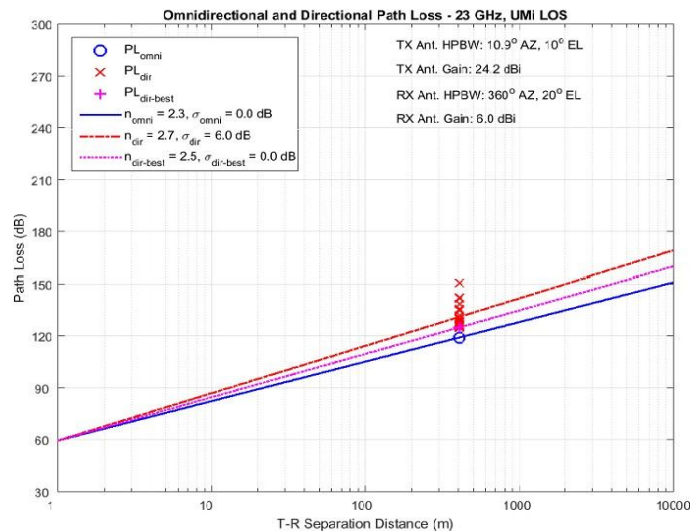


Fig. 2